Electronic Supplementary Information

Nano-SiO_2 Embedded Poly (propylene carbonate)-based Composite Gel Polymer Electrolyte for Lithium-sulfur Batteries

Huijia Huang[a,b], Fei Ding[b,*], Hai Zhong[b], Huan Li[c], Weiguo Zhang[a], Xingjiang Liu[a,b] and Qiang Xu[a,*]

a. School of Chemical Engineering and Technology, Tianjin University, Tianjin, 300072, PR China

b. National Key Lab of Power Sources, Tianjin Institute of Power Sources, Tianjin, 300384, PR China

c. School of Chemical Engineering, The University of Adelaide, Adelaide, 5005, SA, Australia

* Corresponding author. Email: fding@nklps.org (F. Ding) and xuqiang@tju.edu.cn (Q. Xu)

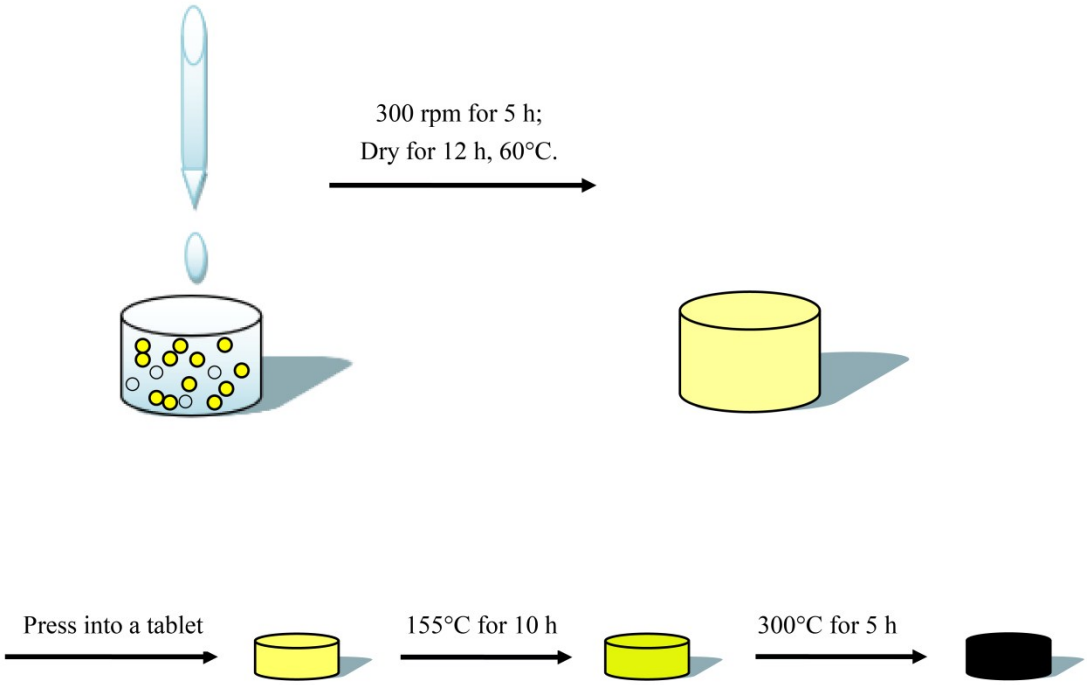

Fig. S1 Schematic of the preparation steps for S/PAN composite. The yellow and white spheres represent sulfur and PAN particles, respectively.

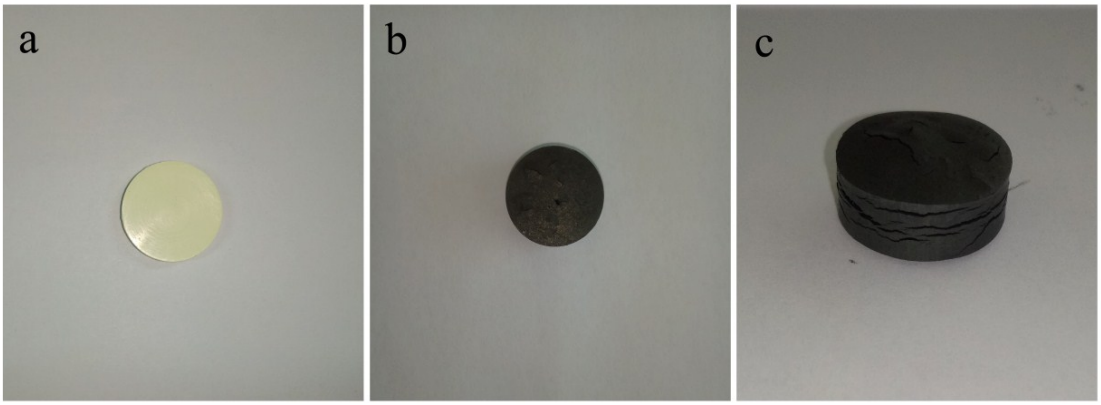

Fig. S2 Digital pictures of (a) the squashed mixture of S and PAN particles and (b, c) the S/PAN composite after being heated.

The morphology and internal structure of S/PAN composite were surveyed by SEM and TEM. As presented in **Fig. S3a** and **b**, the particles of S/PAN composite are closely packed with each other and the average diameter of these particles is about 100-200 nm, which facilitates fast transfer of Li^+ ions and electrons. **Fig. S3c** reveals the structure of S/PAN particles with high magnification. The absence of lattice fringes indicates that element sulfur may exist in form of small sulfur molecules (S_x, $0 < x < 8$),[1-3] which is in accord with XRD results.[4] **Fig. S3d** displays the distribution of C, N and S in S/PAN composite. The element C and N distributed all over the composite particle uniformly, while element S was limited in the interior of material. These results demonstrate that element S had been accommodated in the heterocyclic structure of pyrolytic PAN matrix, which is in conformity with the previous studies.[2, 3, 5]

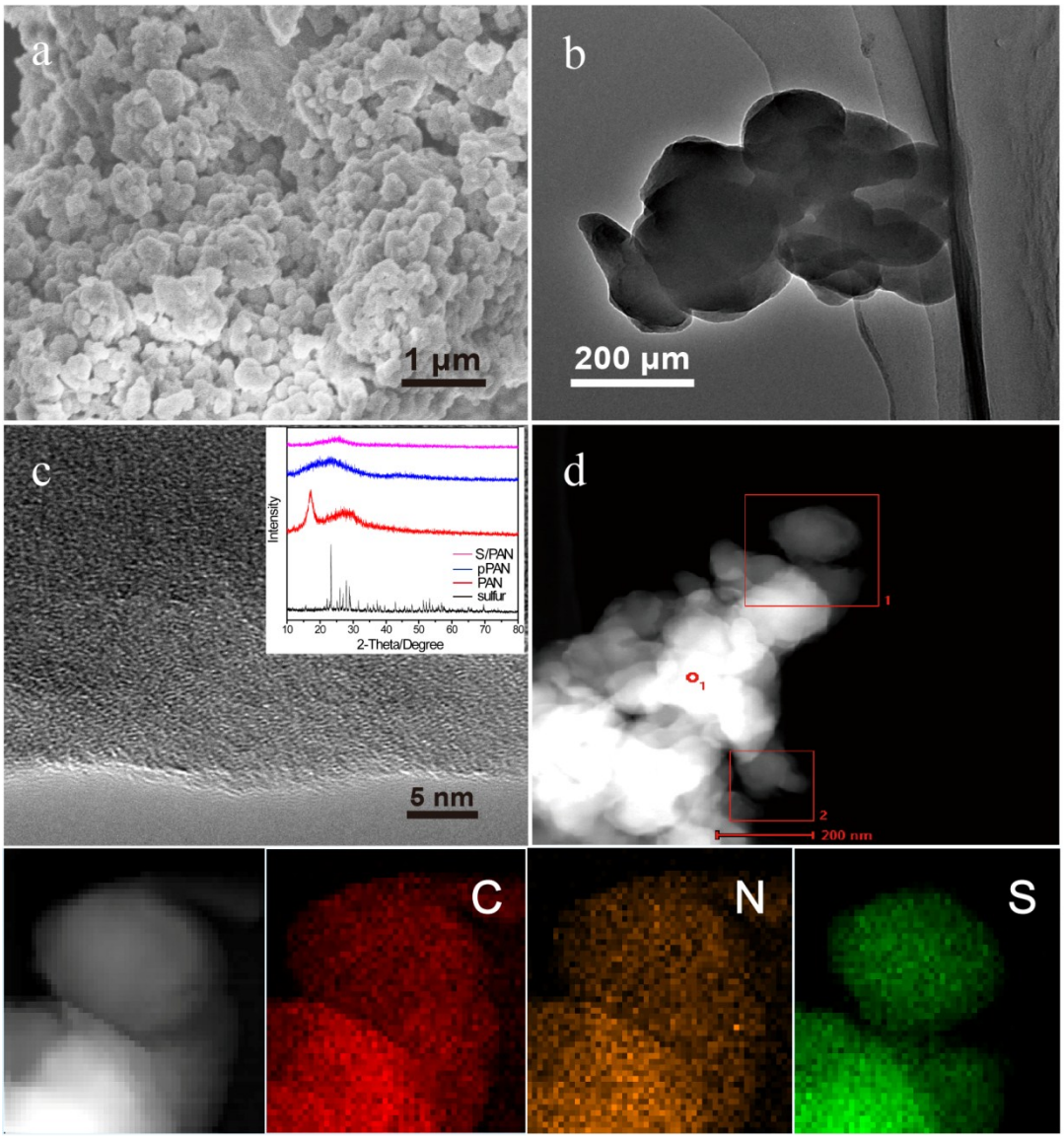

Fig. S3 (a) SEM image of S/PAN composite. (b, c) TEM pictures of S/PAN composite. The inset in (c) is XRD patterns of S/PAN, pyrolytic PAN at 300 °C for 5 h (pPAN), PAN and sulfur. (d) EDS mapping of C, N and S element in the S/PAN composite.

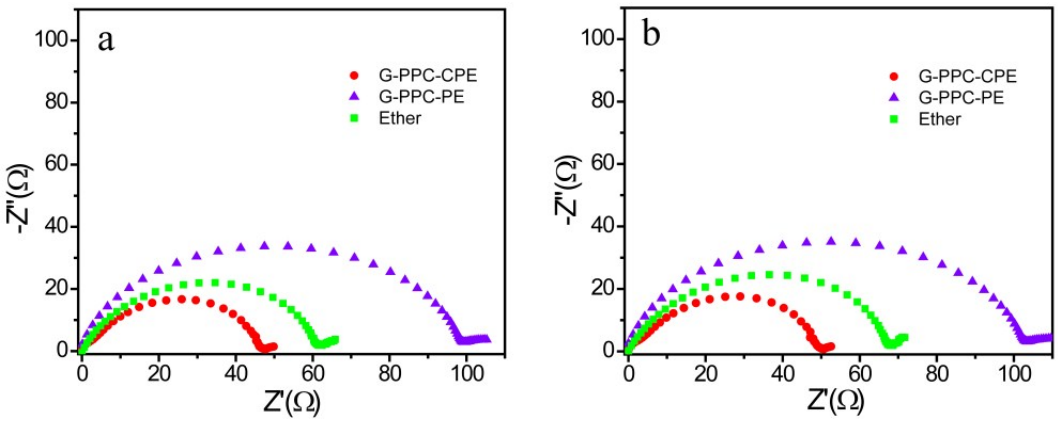

Fig. S4 The recorded Nyquist impedance of Li/electrolyte/Li at (a) initial and (b) steady state.

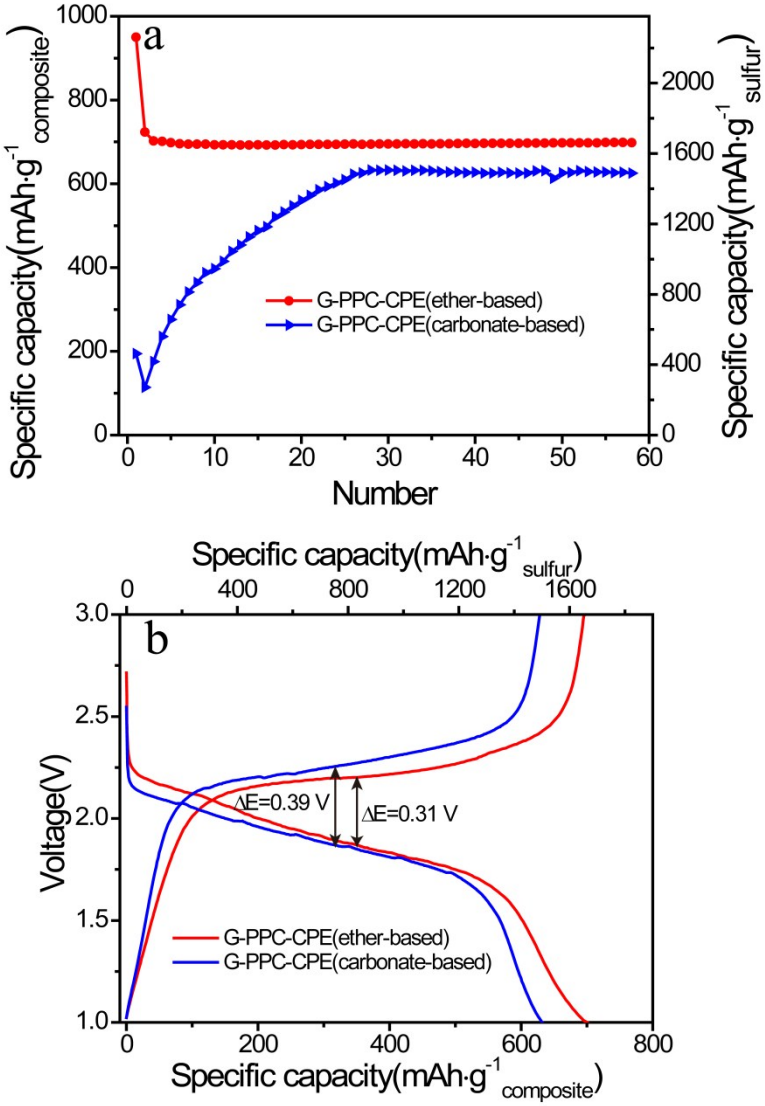

Fig. S5 (a) Discharge capacity vs. cycling number and (b) voltage-capacity profile (during the

cycle 35th) of cell with G-PPC-CPE using the ether-based electrolyte or carbonate-based electrolyte as the plasticizer.

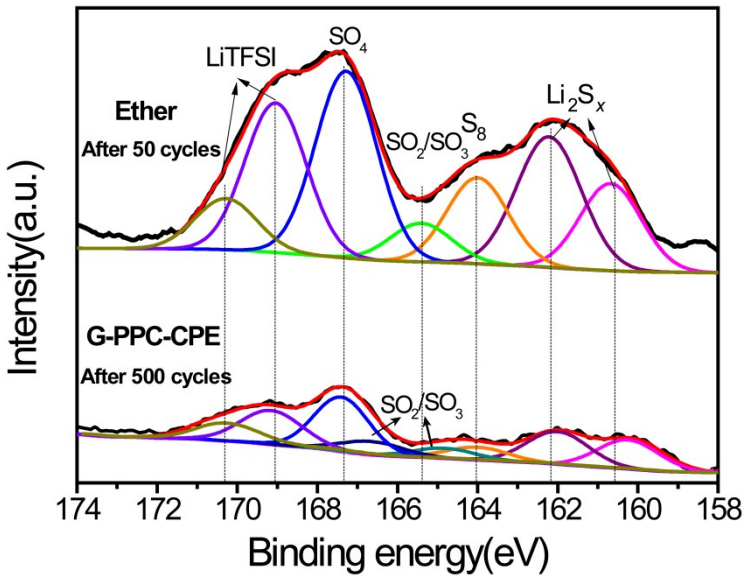

Fig. S6 The XPS spectrum of S 2p on lithium anode disassembled from the LSBs with ether electrolyte cycled for 50 rounds and the LSBs with G-PPC-CPE cycled for 500 rounds at 0.1 $A \cdot g^{-1}$. Peaks at 170.3 and 169.1 eV are assigned to the LiTFSI in the electrolyte.[6] Peaks at 167.3 and 165.4 eV are assigned to SO_4 and SO_2/SO_3 species, respectively.[7] Peaks at 164.0, 162.2 and 160.7 eV are assigned to S_8 and Li_2S_x.[8, 9]

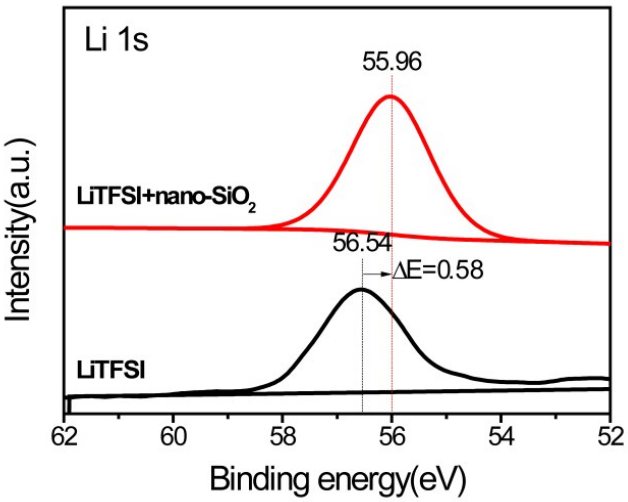

Fig. S7 The XPS spectrum of Li 1S for pure LiTFSI and the mixture of LiTFSI and nano-SiO_2.

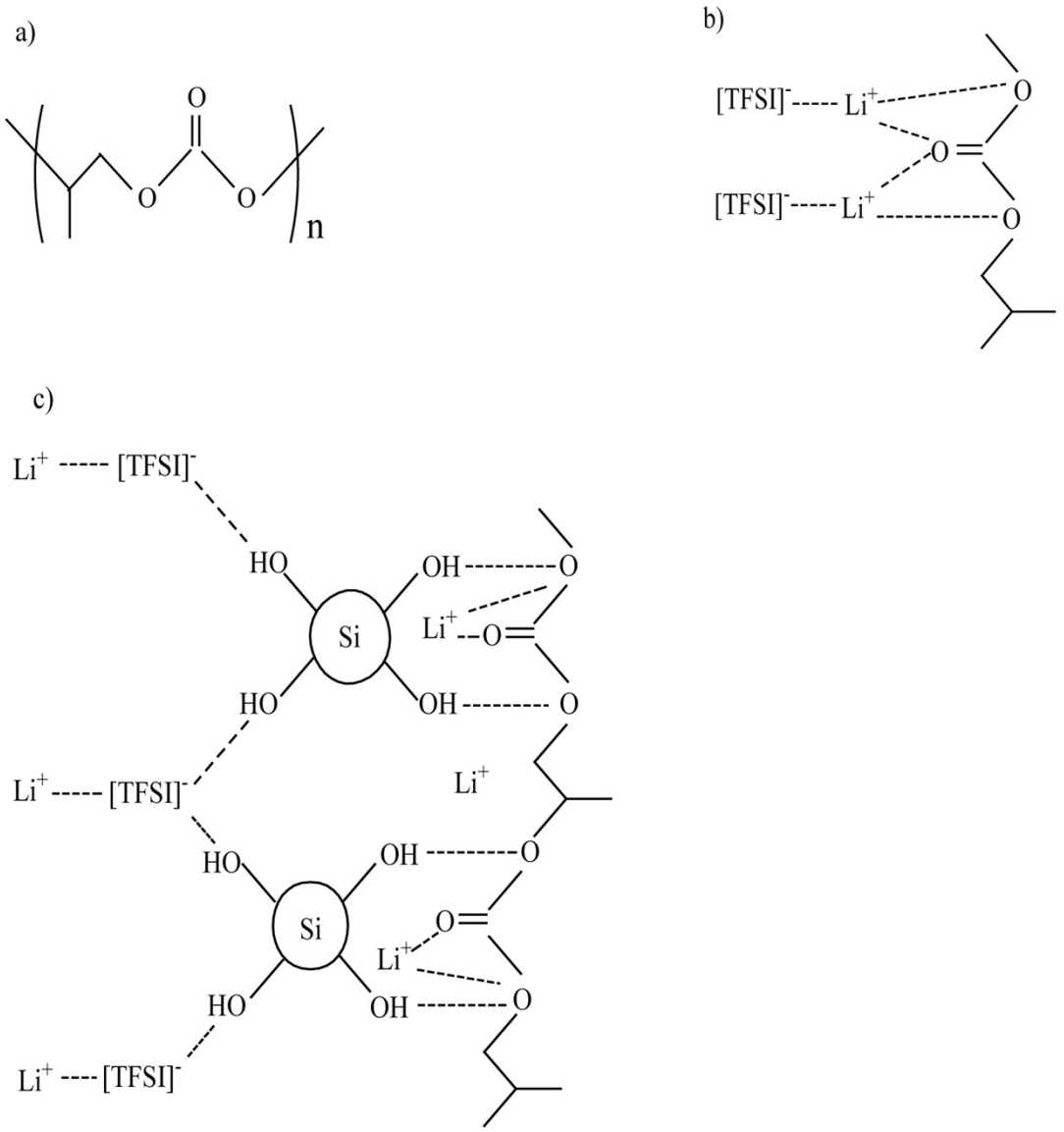

Fig. S8 (a) Structural formula of PPC. Schematic diagrams of (b) the interaction between PPC and LiTFSI in D-PPC-PE and (c) the interaction among PPC, LiTFSI and nano-SiO_2 in D-PPC-CPE.

Table S1 The data obtained from analyses of XPS spectra.

Sample	O 1s			C1s				Si 2p	
	O-C	O=C	O=S/O-Si	C-C	C-O/C-S	C=O	C-F	Si-O	
PPC	533.65	532.13	-	284.64	286.52	290.30	-	-	
LiTFSI	-	-	533.13	-	286.92	-	293.15	-	
nano-SiO_2	-	-	532.83	-	-	-	-	103.57	
D-PPC-PE	533.94	532.35	533.00	284.76	286.59	290.65	292.67	-	
D-PPC-CPE	534.12	532.48	533.05	284.80	286.85	290.81	292.90	I	II
								103.30	101.92

References

1. J. Wang, J. Yang, C. Wan, K. Du, J. Xie and N. Xu, *Adv. Funct. Mater.*, 2003, **13**, 487-492.
2. J. Fanous, M. Wegner, J. Grimminger, Ä. Andresen and M. R. Buchmeiser, *Chem. Mater.*, 2011, **23**, 5024-5028.
3. S. Wei, L. Ma, K. E. Hendrickson, Z. Tu and L. A. Archer, *J. Am. Chem. Soc.*, 2015, **137**, 12143-12152.
4. Y. Zhang, Y. Zhao, A. Yermukhambetova, Z. Bakenov and P. Chen, *J. Mater. Chem. A*, 2013, **1**, 295-301.
5. T. N. L. Doan, M. Ghaznavi, Y. Zhao, Y. Zhang, A. Konarov, M. Sadhu, R. Tangirala and P. Chen, *J. Power Sources*, 2013, **241**, 61-69.
6. J. Zheng, M. Gu, H. Chen, P. Meduri, M. H. Engelhard, J.-G. Zhang, J. Liu and J. Xiao, *J. Mater. Chem. A*, 2013, **1**, 8464.
7. M. Liu, D. Zhou, Y.-B. He, Yongzhu Fuc, X. Qin, C. Miao, H. Du, B. Li, Q.-H. Yang, Z. Lin, T. S. Zhao and F. Kang, *Nano Energy*, 2016, **22**, 278–289.
8. R. Demir-Cakan, M. Morcrette, Gangulibabu, A. Guéguen, R. Dedryvère and J.-M. Tarascon, *Energy & Environ. Sci.*, 2013, **6**, 176.
9. H. Liao, H. Wang, H. Ding, X. Meng, H. Xu, B. Wang, X. Ai and C. Wang, *J. Mater. Chem. A*, 2016, **4**, 7416-7421.